Oil Well Diagnosis by Sensing Terminal Characteristics of the Induction Motor

Bogdan M. Wilamowski, *Fellow, IEEE,* and Okyay Kaynak, *Senior Member, IEEE*

***Abstract*—Oil well diagnosis usually requires dedicated sensors placed on the surface and the bottom of the well. There is significant interest in identifying the characteristics of an oil well by using data from these sensors and neural networks for data processing. The purpose of this paper is to identify oil well parameters by measuring the terminal characteristics of the induction motor driving the pumpjack. Information about oil well properties is hidden in instantaneous power waveforms. The extraction of this information was done using neural networks. For the purpose of training neural networks, a complex model of the system, which included 25 differential equations, was developed. Successful application of neural networks was possible due to the proposed signal preprocessing which reduces thousands of measured data points into 20 scalar variables. The special input pattern transformation was used to enhance the power of the neural networks. Two training algorithms, originally developed by authors, were used in the learning process. The presented approach does not require special instrumentation and can be used on any oil well with a pump driven by an induction motor. The quality of the oil well could be monitored continuously and proper adjustments could be made. The approach may lead to significant savings in electrical energy, which is required to pump the oil.**

***Index Terms*—Induction motor, neural networks, oil well.**

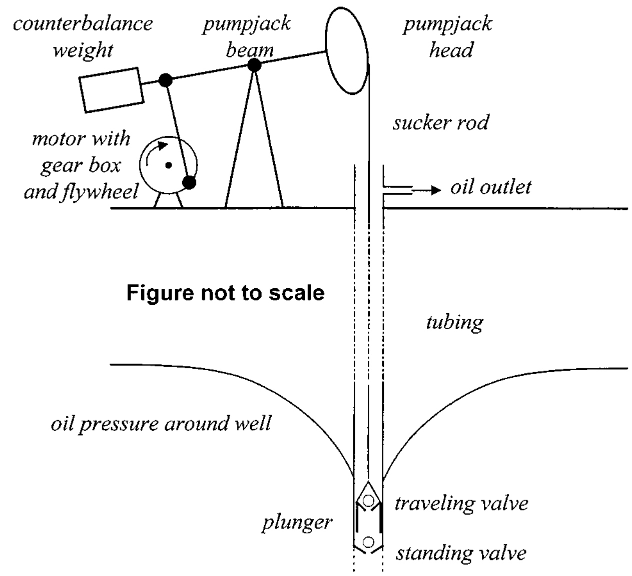

Fig. 1. Schematic sketch of an oil well with pump jack.

I. Introduction

OIL WELL diagnosis usually requires sophisticated tools and introduces specialized sensors placed on the surface and the bottom of the well [1], [2]. Recently, there is significant interest in identifying characteristics of oil wells using neural networks [3]–[14]. All of the described approaches use information from special sensors. The purpose of this approach is to use the information from the terminal characteristics of the induction motor that drives the pumpjack. Neural networks are already successfully used for fault identification of electrical motors [15]–[21].

With the presented approach, the quality of the oil well could be monitored continuously and proper adjustments could be made. This approach may lead to significant savings in electrical energy, which is required to pump the oil. With this approach, motors with smaller nominal power can be used instead of overrated motors operating at a fraction of their nominal power. The application of this new technology could lead to constant and effective monitoring of oil wells. These measurements may lead to better diagnosis, adjustment, choice for an optimum pumping rate, and more efficient use of energy.

It is not economically justified to introduce faults in real oil wells. Therefore, for the purpose of generating training patterns, a complex model of oil well was developed. This model is described in Section II. Section III is devoted to numerical simulation. Section IV describes the data preprocessing and compression. Section V presents neural network architecture and input data transformation, which leads to easy separation of clusters. Section VI includes results of identification of specific faults.

II. Oil Well Model

The model of the pumpjack and the oil well is relatively complex. A schematic diagram of the oil well is shown in Fig. 1. The entire system is described by a 25th-order system of differential equations and 25 state variables. Both the induction motor and the gearbox with jack introduce relatively complex nonlinear systems, which require numerical solutions. A more detailed description of the different portions of this model is given in this section.

A. Model of Induction Motor

For the induction motor, a third-order IEEE standard model was used. Since oil wells are usually located in remote places, the standard model of an induction motor was enhanced with several additional elements such as R_S, R_L, and X_L, which

Manuscript received January 15, 1999; revised April 29, 2000. Abstract published on the Internet July 1, 2000.

B. M. Wilamowski is with the College of Engineering, University of Idaho, Boise, ID 83712 USA (e-mail: wilam@ieee.org).

O. Kaynak is with the Electrical and Electronic Engineering Department, Bogazici University, Bebek, 80815 Istanbul, Turkey (e-mail: kaynak@boun.edu.tr).

Publisher Item Identifier S 0278-0046(00)08841-9.

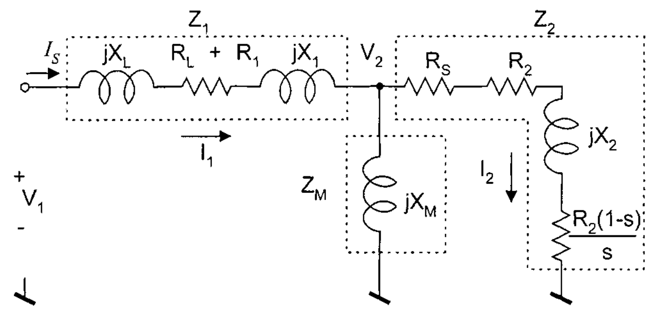

Fig. 2. Equivalent diagram of induction motor with transmission lines.

represent additional loses, transmission line resistance, and inductance, respectively. The equivalent diagram of an induction motor with transmission lines is shown in Fig. 2.

The mesh currents I_1 and I_2 are given by

$$I_1 = V_1 \frac{1 + \frac{Z_2}{Z_M}}{Z_1 + Z_2 + \frac{Z_1 Z_2}{Z_M}} \quad I_2 = \frac{V_1}{Z_1 + Z_2 + \frac{Z_1 Z_2}{Z_M}}. \tag{1}$$

Input complex power and output torque are

$$P_1 = V_1 I_1^* \quad T = \frac{P_2}{2\pi f_s}. \tag{2}$$

The real power delivered to load is

$$P_2 = \frac{R_2(1-s)}{s} I_2^2 \tag{3}$$

where s is the slip, $f_o = 60$ Hz, and $f_s = f_o(1-s)$.

Using the above relations, the input powers and slip can be computed numerically as a function of the output torque. Fig. 3 shows this relation for the 10-kW motor with the following parameters: $V_1 = 120\ \mathrm{V_{RMS}}, R_L = 0.1, X_L = j0.1, R_1 = 0.45, X_1 = j0.76, X_M = j28, R_2 = 0.4, X_2 = j0.76$, and $R_S = 0.1$.

B. Model of Gearbox With Jack

The gearbox and jack are described by four state variables: the angular flywheel velocity, angular flywheel acceleration, beam angle, and beam angular velocity. Note that a relatively complex nonlinear relationship exists between the angular position of the gear flywheel and the angular position of the pumpjack beam. For the geometry shown in Fig. 4 the following relationships are valid:

$$\begin{aligned} y &= r\sin(\alpha) + y_0 \\ x &= r\cos(\alpha) + x_0 \end{aligned} \tag{4}$$

$$\begin{aligned} Y_1 &= -R_1\sin(\beta) + Y_0 \\ X_1 &= -R_1\cos(\beta) + X_0 \end{aligned} \tag{5}$$

$$(Y_1 - y)^2 + (X_1 - x)^2 = d^2. \tag{6}$$

By inserting (4) and (5) into (6) and after several manipulations, one can obtain (7), shown at the bottom of the page. This equation can be easily solved numerically using the Gauss–Seidl approach. The sucker rod displacement

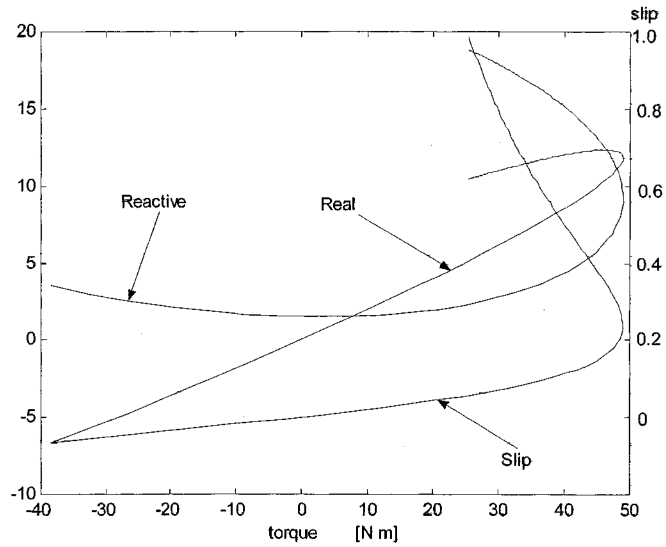

Fig. 3. Slip, and input real and reactive powers as a function of the output torque for the 10-kW induction motor.

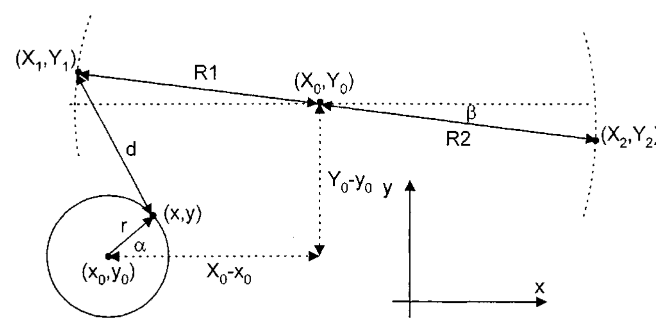

Fig. 4. Pump jack geometry.

$$\Delta y = R_2 \beta \tag{8}$$

is proportional to angle β which is an implicit function of the rotation angle α. The Δy can be approximated by

$$\Delta y = r\frac{R_2}{R_1}\sin(\alpha + \alpha_0). \tag{9}$$

The approximate solution gives a pure sinusoidal relationship, while the actual relationship is a distorted sinusoid, as shown in Fig. 5. The differences between actual and approximate relationships are shown in Fig. 6. For both figures, Figs. 5 and 6, the following geometrical parameters, as shown in Fig. 4, were used: $r = 0.7$ m, $R_1 = 2$ m, $R_2 = 3$ m, $x_0 = 1$ m, $y_0 = 1$ m, $X_0 = 3$ m, $Y_0 = 3.3$ m, and $d = 1.8$ m.

Since the shape of instantaneous power on the induction motor terminals carries important information about the properties of the oil well, the actual relationships must be used. This again requires a numerical solution.

$$\sin(\beta) = \frac{Y_0 - y_0 - r\sin(\alpha) - \sqrt{d^2 - [R_1\sqrt{1-\sin^2(\beta)} + r\sqrt{1-\sin^2(\alpha)} + x_0 - X_0]^2}}{R_1} \tag{7}$$

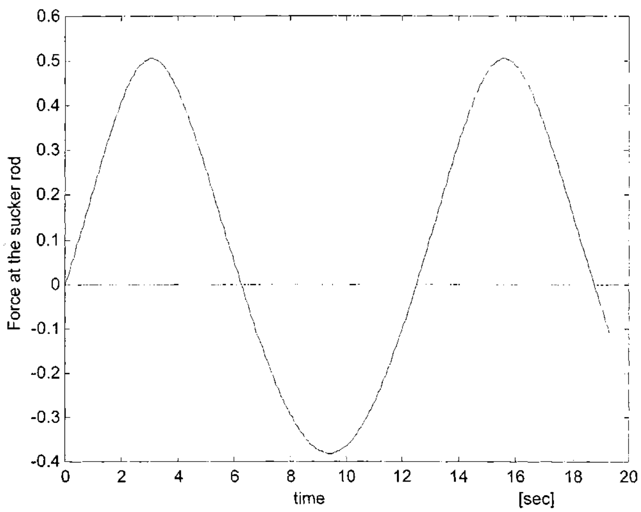

Fig. 5. Force at the top of the sucker rod as a function of time (rotation angle α).

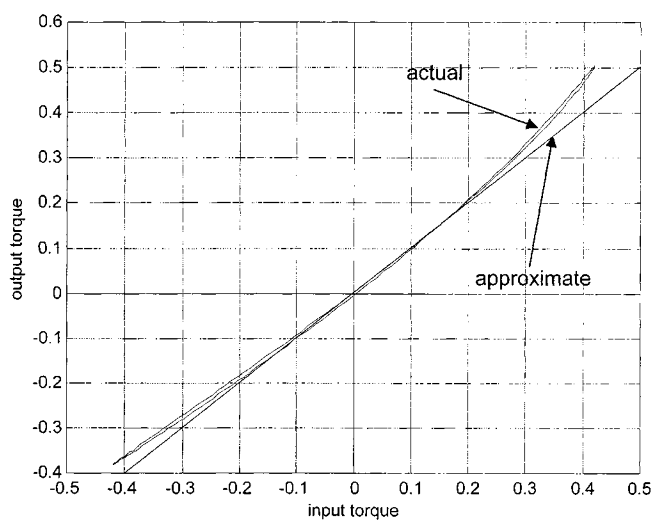

Fig. 6. Nonlinearity of the gearbox with jack.

C. Model of Sucker Rod With Plunger

For deep wells, the diameter of the sucker rod changes and this leads to different stiffness and different mass for every section of sucker rod. This distributed parameter system can be properly approximated by lumped eight state variable systems representing displacement and velocities of sucker rod sections. Oil flow in the tube can be modeled by two additional state variables representing displacement and velocity. The model of the sucker rod with plunger, which is shown in Fig. 7, is described by the following set of eight differential equations:

$$\frac{dv_1}{dt} = g - \frac{k_0(x_1 - x_0) + b_1 v_1 + k_1(x_1 - x_2)}{m_1} \tag{10}$$

$$\frac{dx_1}{dt} = v_1 \tag{11}$$

$$\frac{dv_2}{dt} = g - \frac{k_1(x_2 - x_1) + b_2 v_2 + k_2(x_2 - x_3)}{m_2} \tag{12}$$

$$\frac{dx_2}{dt} = v_2 \tag{13}$$

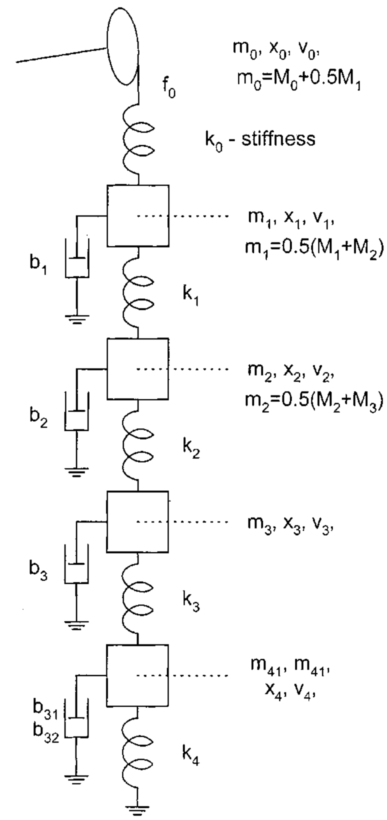

Fig. 7. Model of sucker rod with plunger.

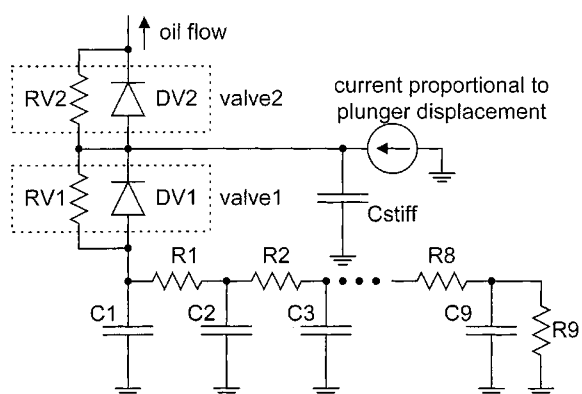

Fig. 8. Model of oil flow in formation and through valves.

$$\frac{dv_3}{dt} = g - \frac{k_2(x_3 - x_2) + b_3 v_3 + k_3(x_3 - x_4)}{m_3} \tag{14}$$

$$\frac{dx_3}{dt} = v_3 \tag{15}$$

$$\begin{aligned}\frac{dv_4}{dt} &= 0.5[1 + \tanh(100 v_4)]\left(g - \frac{k_3(x_4 - x_3) + b_{41} v_4}{m_{41}}\right)\\ &\quad + 0.5[1 - \tanh(100 v_4)]\\ &\quad \times \left(g - a p_{\text{well}} - \frac{k_3(x_4 - x_3) + b_{42} v_4}{m_{42}}\right)\end{aligned} \tag{16}$$

$$\frac{dx_4}{dt} = v_4. \tag{17}$$

The last segment of the model, which is described by (16), has a relatively complex formula, which is different for the positive and negative velocity of the plunger. With upward velocity,

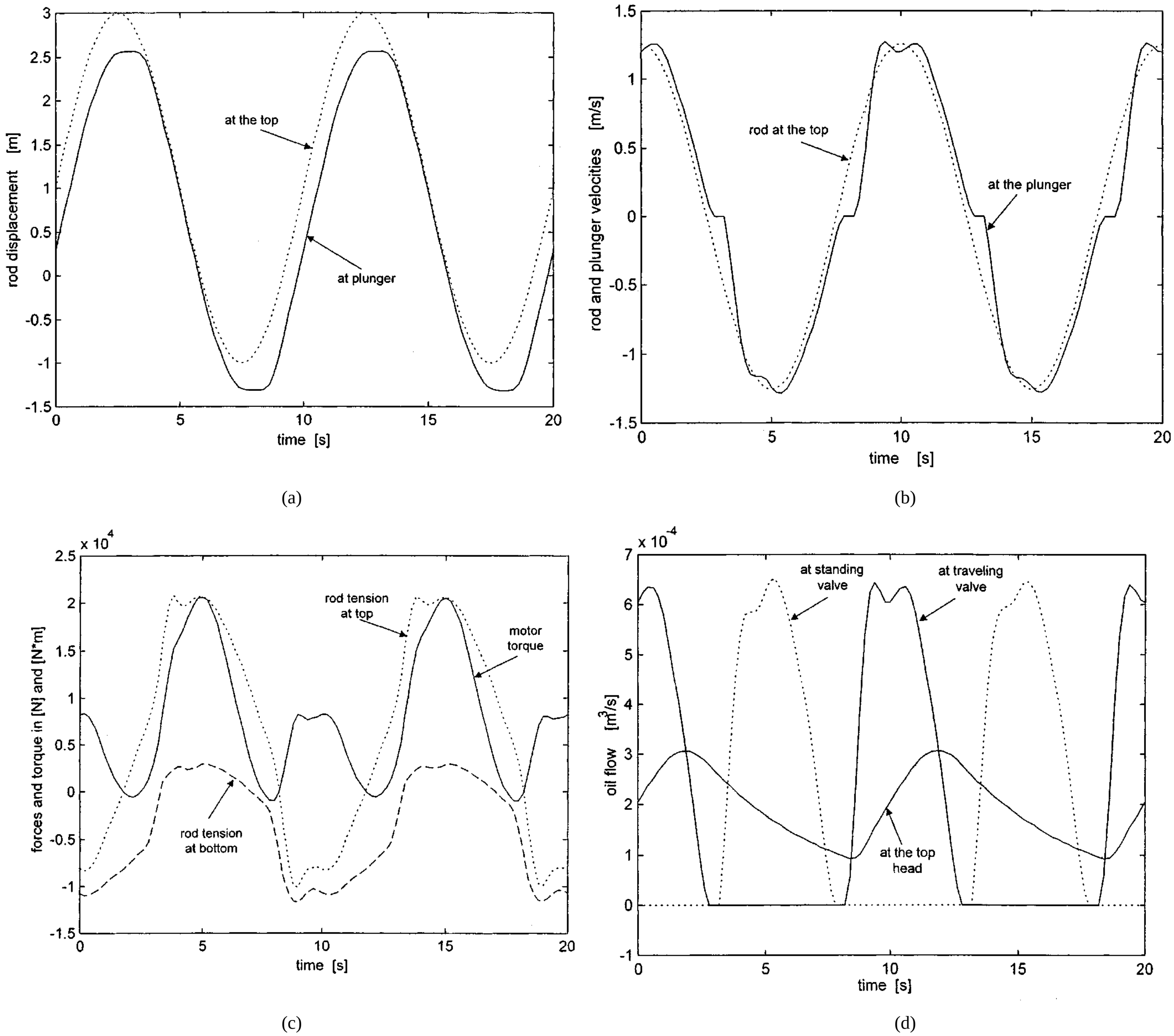

Fig. 9. Results of simulation of the 1500-m-deep oil well where pumpjack balance mass is not chosen properly. (a) Sucker rod displacements. (b) Sucker rod velocities. (c) Forces and torques. (d) Oil flow.

both the mass of the sucker rod and the mass of the oil in the pipe must be encountered. Depending on the velocity direction, the different frictional losses must be included. During the upward movement, additional force due to the existence of differential pressure must be also incorporated. Instead of signum function, a hyperbolic tangent was used in order to secure the numerical stability. Note that the differential pressure parameter $p_{\rm well}$ depends on the depth of the oil table.

D. Model of Three Dimensional Flow in the Formation

A three-dimensional model of oil flow through the formation can describe oil pressure distribution around the well. If radial uniformity is assumed, this problem can be reduced to a one-dimensional distributed parameter case, which can be well approximated with ten state variables representing oil pressure for different distances from the well, as shown in Fig. 8.

III. Generation of Training Patterns for Neural Networks

There are very different time constants in the system. The smallest time constants, which are associated with the induction motor and sucker rod dynamics, are in the range of milliseconds. The pumpjack operates with cycles varying from 5 to 20 s. Transient responses in the well itself have time constants from several hours to several weeks, or even years, when well capacity is considered. Significant differences in time constants make the system very stiff and difficult to analyze. Traditional forward Euler or Runge–Kutta methods would require the use of very small time steps and an unrealistically long simulation time. Many electronic systems have a similar stiffness and it is usually solved by either trapezoidal or Gear methods. Both are implicit methods. At each iteration step the system is linearized and a solution to the set of linear equations must be found. Both schemes are also used in the popular Spice program [22]. Since

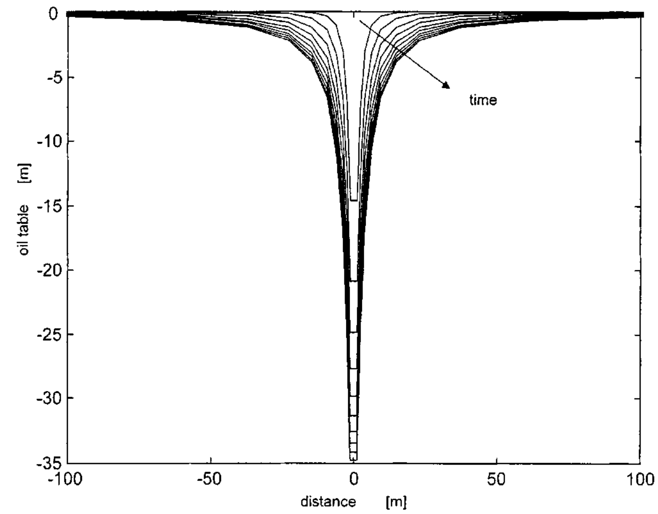

(a)

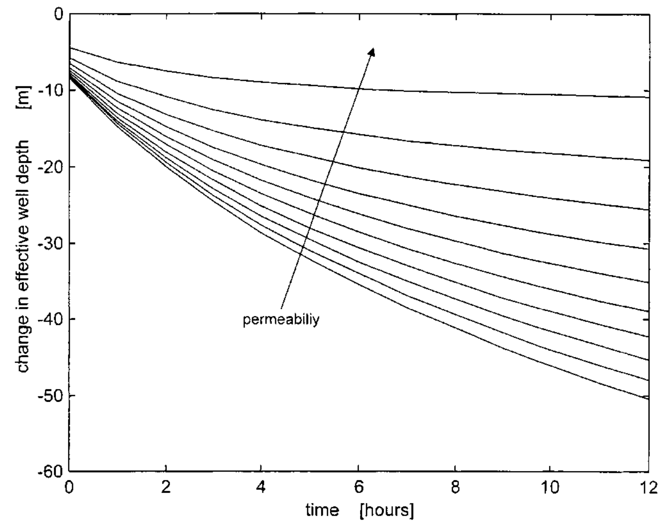

(b)

Fig. 10. Oil pressure distribution in vicinity of the well. (a) spatial distribution around well with pumping time as parameter. (b) Transient response of the pressure in the well with soil permeability as parameter.

the use of the implicit integration scheme, the computation time is almost independent of the observation time.

The system of 25 differential equations is relatively complex, but the simulation time for one set of parameters is usually completed within 15–30 s on a Pentium 200-MHz computer. When the transient response of the well was done for a very large observation time (hours or weeks), then the complex 25th-order model was replaced with a simpler model by replacing pulsed oil flow with steady flow. With this simplification, the simulation is done within 1 min, even for observation times of several weeks.

Sample results of oil well simulations using the complex model are shown in Fig. 9. Fig. 10 illustrates the oil table change as a function of pumping time. Other data for faulty traveling valve are given in [14]. The developed model of the oil well was then used to generate data required for neural network training.

The recording of currents and voltages at terminals of the three-phase induction motor operating at 60 Hz leads to the collection of a tremendous amount of data. It turns out that most of the important information is contained in the instantaneous power of the induction motor [19]. The data for the transient waveform of the instantaneous power is processed with a fast Fourier transform (FFT). The complex Fourier coefficients are generated, as shown in Fig. 11. Since this mechanical system includes several large masses with inertia, the system works as a high-order low-pass filter, therefore, only the first nine Fourier components are used. As a result, each instantaneous power waveform is represented by 20 numeric values: nine real, nine imaginary, one representing the fundamental frequency, and one representing the dc offset. These 20 values were used as the input pattern for the neural network.

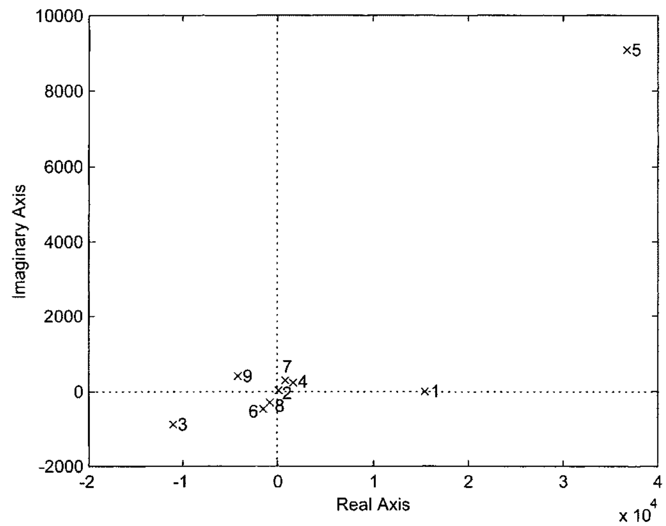

Fig. 11. Instantaneous power waveform represented by complex Fourier coefficients.

IV. Neural Network Architecture and Training

Two different neural network architectures were used. For the purpose of function approximation, the standard sigmoidal feedforward neural network was used, and for the fault diagnosis, a special neural network architecture was implemented as described later in this section.

In order to identify the depth of the oil table, the three-layer standard feedforward network was used as a general approximator with one output. Various feedforward structures were explored with one pattern file used for training and with another pattern file used for verification. All input and output patterns were scaled in such a way that input and output values changed within the -1 to $+1$ range. The best compromise between accuracy and generalization was obtained using a neural network with one hidden layer and full connections across layers. This network has 20 inputs, ten neurons in the hidden layer, and one output neuron. To train the network, a specially developed algorithm described in [23] was used. This algorithm has the advantage of rapid convergence of the Levenberg–Marquardt (LM) algorithm [24], but in contrast to the LM algorithm it also works well for large network structures.

The feedforward network 21-10-1 was adequate for function approximation, but it was found impractical for the iden-

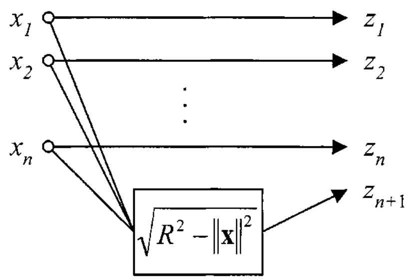

Fig. 12. Transformation of input patterns to $n+1$ dimensional space.

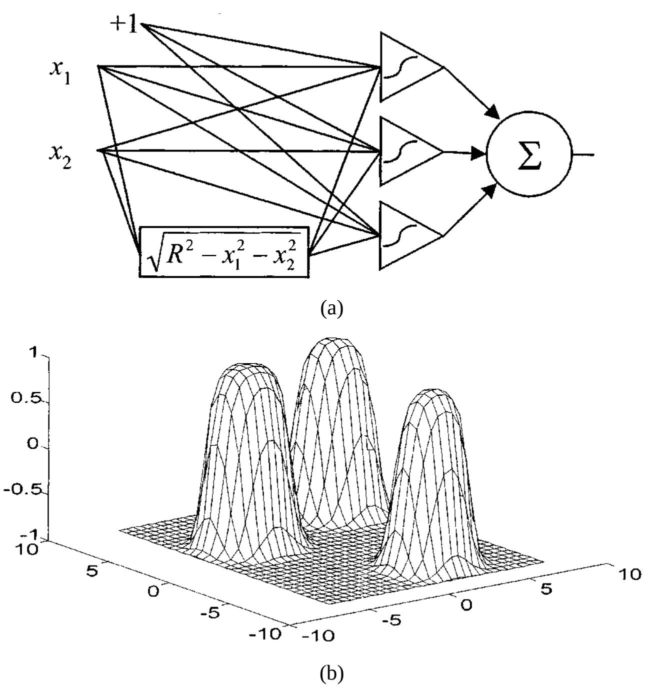

Fig. 13. Example of cluster separation in two-dimensional input space using input pattern transformation to $n+1$ dimensional space. (a) Network architecture. (b)Transfer function of the network.

tification of faults such as the leakage of the traveling valve, the leakage of the standing valve, and the mass misbalance on the beam. Each abnormal mode of operation usually formed a cluster of patterns in multidimensional input space, and these clusters are specific to a given abnormality. In order to select just one region in the n-dimensional input space, more than $n+1$ neurons in the input layer should be used. Radial base function (RBF) neurons [25], [26] are able to separate patterns in the input space by circle, sphere, and hypersphere. This feature makes the RBF network very simple and powerful in pattern recognition. Unfortunately, RBF networks are difficult to train. When the relatively simple transformation [27] to $n+1$ dimensional space

$$z_i = \begin{cases} x_i, & i = 1, 2, \ldots, n \\ \sqrt{R^2 - \|\mathbf{x}\|^2}, & i = n+1 \end{cases} \tag{18}$$

is done to the input patterns as shown in Fig. 12, then the feedforward neural network with simple neurons can separate clusters in the input space by circle, sphere, and hypersphere. For example, after the transformation given by (18), three clusters in a two-dimensional input space can be easily separated by three sigmoidal neurons as shown in Fig. 13. With the introduced transformation, a neural network with only one layer can be used. Such network can be very easily trained. In our case, the modified regression algorithm, as described in [28], was used.

V. Results

Initially, both training patterns and verification patterns were generated in such a way that, for each pattern, only one variable (for example, leakage of the traveling valve) was modified and the remaining parameters had normal values. In this case, the neural network was able to identify the correct fault in 100% of cases. More importantly, the neural network was also able to identify how much a certain parameter had deteriorated. For example, what is the leakage? What is the effective depth? What is the location of the balance mass? The accuracy of this identification varied from 10%, in the case of the effective oil depth, to 50%, in the case of the standing valve leakage.

For the next experiment, all four faults were introduced simultaneously by randomly chosen values. In this experiment, correct results were obtained only if there was one clearly dominant fault. When several faults were present, then the neural network was often confused and misidentified faults. This means that there are strong interactions of a nonlinear nature between the parameters. This part would require further study and probably a more sophisticated neural network architecture. Introduction of other inputs to the network, which can be easily measured on the surface, such as tension of the sucker rod, may help.

Fortunately, three out of four of the investigated parameters (the leakages and the mass location) can be assumed constant during experiments, which leads to the identification of formation permeability and reservoir capacity. As Fig. 10(a) shows, the pressure distribution around a well changes with the pumping time. The only parameter, which can be observed in the wellbore, is the effective depth of the oil table. Fig. 10(b) shows how the effective oil depth changes with time for different values of the formation permeability. From such transient responses it is possible, using well-established techniques [29]–[31], to estimate formation permeability and drainage-area pressure, reservoir heterogeneity, or boundaries. In the traditional approach, the test is conducted by pumping oil at a constant rate for some time, shutting down the pump, allowing the pressure to build up in the wellbore, and recording the pressure in the wellbore as a function of time. This, of course, requires a pressure sensor located at the bottom of the well. Note that, with neural network diagnosis, the effective depth of the well (pressure) can be identified from terminal parameters of the induction motor and this can be used instead of a special sensor at the bottom of the well. The proposed approach differs from the traditional in that the pressure can be measured only when the pump is active.

VI. Conclusion

The terminal parameters of the induction motor contain significant information about the oil well, which can be extracted using neural networks. This information is not only about the condition of the oil reservoir, but it may lead to better adjustments of the pump and its ballast so the pumping can be done more efficiently. With this approach, motors with smaller nominal power can be used instead of overrated motors operating at a fraction of their nominal power. The application of this new technology could lead to constant and effective monitoring of oil wells. Measurements may lead to better diagnosis, adjustment, choice of the optimum pumping rate, and a more efficient use of energy.

REFERENCES

[1] T. Chakrabarty, "A new robust algorithm for rapid determination of porosity and lithology from well logs," in *47th CIM Petroleum Society Annu. Technical Meeting Preprints*, vol. 1, Paper CIM 96-17. Calgary, AB, Canada, 1996, p. 15.

[2] B. Braunschweig and R. Day, "Prolegomena—An overview of AI techniques and of their use in the petroleum industry," in *Artificial Intelligence in the Petroleum Industry*, Paris, France: Pennwell, 1995, vol. 1, pp. 2–37.

[3] G. B. Arpat, "Prediction of permeability from wire-line logs using artificial neural networks," in *Proc. Annu. Tech. Conf. and Exhibition, V. Omega, Formation Evaluation and Reservoir Geology*, 1997, pp. 531–537.

[4] B. Baygun, S. M. Luthi, and I. D. Bryant, "Applications of neutral networks and fuzzy logic in geological modeling of a mature hydrocarbon reservoir," in *Artificial Intelligence in the Petroleum Industry*. Paris, France: Pennwell, 1996, vol. 2, ch. 5, pp. 125–138.

[5] A. Bonarini, A. Corrao, L. Giacometti, and L. Tomada, "A fuzzy logic enhancement to a support system for the recognition of sedimentary environments from core analysis," in *Artificial Intelligence in Petroleum Industry*, Paris, France: Pennwell, 1995, vol. 1, ch. 12, pp. 2–37.

[6] A. Chawathe, A. Ounes, and W. Weiss, "Predicting unconventional well logs from conventional well logs using neural networks," *In Situ*, vol. 21, no. 2, pp. 145–159, 1997.

[7] C. A. Gonclaves, P. K. Harvey, and M. A. Lovell, "Prediction of petrophysical parameter logs using a multilayer backpropagation neural network," in *Developments in Petrophysics: Geological Society Special Publication*. London, U.K.: Geological Society, 1997, pp. 169–180.

[8] S. M. Luthi and I. D. Bryant, "Well-log correlation using a back-propagation neural network," *Math. Geology*, vol. 29, no. 3, pp. 413–425, 1997.

[9] S. Mohaghegh, R. Arefi, S. Ameri, K. Aminiand, and R. Nutter, "Petroleum reservoir characterization with the aid of artificial neural networks," *J. Petrol. Sci. Eng.*, vol. 16, no. 4, pp. 263–274, 1996.

[10] M. N. Panda, D. E. Zuacha, G. Perez, and A. K. Chopra, "Application of neural networks to modeling fluid contacts," *Soc. Petrol. Eng. J.*, vol. 1, no. 3, pp. 303–311, 1996.

[11] A. Schumann, "Neural networks versus statistics—A comparing study of their classification performance on well log data," in *Proc. 3rd Annu. Conf. International Association for Mathematical Geology—IAMG'97*, Barcelona, Spain, 1997, pp. 237–241.

[12] N. Shimada, A. Tani, and N. Nishikawa, "Reservoir characterization using artificial neural networks," in *Proc. 3rd Well Logging Symp. Japan: Society of Professional Well Log Analysts*, 1997, p. 6.

[13] P. M. Wong, D. J. Henderson, and L. J. Brooks, "Reservoir permeability determination from well log data using artificial neural networks—An example from the Ravva field, offshore India," in *Conf. Proc. Asia Pacific Oil and Gas: Society of Petroleum Engineers*, SPE-38 034, 1997, pp. 149–155.

[14] B. M. Wilamowski, "Faults identification of oil wells using neural networks," in *Proc. Int. Conf. Recent Advances in Mechatronics—ICRAM'99*, Istanbul, Turkey, May 24–26, 1999, pp. 459–467.

[15] M.-Y. Chow, R. N. Sharpe, and J. C. Hung, "On the application and design of artificial neural networks for motor fault detection—Parts I and II," *IEEE Trans. Ind. Electron.*, vol. 40, pp. 181–197, Apr. 1993.

[16] P. V. Goode and M.-Y. Chow, "Using a neural/fuzzy system to extract knowledge of incipient fault in induction motors—Parts I and II," *IEEE Trans. Ind. Electron.*, vol. 42, pp. 131–146, Apr. 1995.

[17] M.-Y. Chow, *Methodologies of Using Artificial Neural Network and Fuzzy Logic Technologies for Motor Incipient Fault Detection*, Singapore: World Scientific, 1997.

[18] F. Filipetti, G. Franchescini, and C. Tassoni, "Neural networks aided on-line diagnostics of induction motor faults," *IEEE Trans. Ind. Applicat.*, vol. 31, pp. 892–899, July/Aug. 1995.

[19] S. F. Legowski, A. H. M. S. Ula, and A. M. Trzynadlowski, "Instantaneous power as a medium for the signature analysis of induction motors," *IEEE Trans. Ind. Applicat.*, vol. 32, pp. 904–909, July/Aug. 1996.

[20] R. R. Schoen, B. K. Lin, T. G. Habetler, J. H. Schlag, and S. Farag, "An unsupervised, on-line system for induction motor fault detection using stator current monitoring," *IEEE Trans. Ind. Applicat.*, vol. 31, pp. 1280–1286, Nov./Dec. 1995.

[21] F. C. Trutt, C. S. Cruz, J. L. Kohler, and J. Sittuke, "Prediction of electrical behavior in deteriorating induction motors," *IEEE Trans. Ind. Applicat.*, vol. 29, pp. 1239–1243, Nov./Dec. 1993.

[22] B. M. Wilamowski and R. C. Jaeger, *Computerized Circuit Analysis Using SPICE Programs*. New York: McGraw-Hill, 1997.

[23] B. M. Wilamowski, Y. Chen, and A. Malinowski, "Efficient algorithm for training neural networks with one hidden layer," in *Proc. 1999 Int. Joint Conf. Neural Networks—IJCNN'99*, Washington, DC, July 10–16, 1999, pp. 1725–1728.

[24] M. T. Hagan and M. Menhaj, "Training feedforward networks with the Marquardt algorithm," *IEEE Trans. Neural Networks*, vol. 5, pp. 989–993, Nov. 1994.

[25] J. Moody and C. J. Darken, "Fast learning networks of locally-tuned processing units," *Neural Comput.*, vol. 1, no. 2, pp. 281–294, 1989.

[26] E. Hartman, J. D. Keeler, and J. M. Kowalski, "Layered neural networks with Gaussian hidden units as universal approximations," *Neural Comput.*, vol. 2, no. 2, pp. 210–215, 1990.

[27] B. M. Wilamowski and R. C. Jaeger *et al.*, "Implementation of RBF networks by feedforward sigmoidal neural networks," in *Intelligent Engineering Systems Through Artificial Neural Networks*, C. H. Dagli, *et al. et al.*, Eds. New York: ASME Press, 1997, vol. 7, pp. 183–188.

[28] T. J. Andersen and B. M. Wilamowski, "A. modified regression algorithm for fast one layer neural network training," in *Proc. World Congr. Neural Networks*, vol. 1, Washington, DC, July 17–21, 1995, pp. 687–690.

[29] D. R. Horner, "Pressure buildup in wells," in *Proc. Third World Petroleum Conf.*, The Hague, The Netherlands, 1951, pp. 503–523.

[30] ——, *Pressure Analysis Methods*. Dallas, TX: SPE, 1967, vol. 9, pp. 25–43.

[31] W. M. Cobb and J. T. Smith, "An investigation of pressure buildup test in bounded reservoirs," *J. Petrol. Technol.*, pp. 991–996, Aug. 1975.

Bogdan M. Wilamowski (SM'83–F'00) received the M.S. degree in computer engineering, the Ph.D. degree in neural computing, and the Dr.Habil. degree in integrated circuit design from the Technical University of Gdansk, Gdansk, Poland, in 1966, 1970, and 1977, respectively.

He received the title of Professor from the President of Poland in 1987. He was the Director of the Institute of Electronics (1979–1981) and the Chair of the Solid State Electronics Department (1987–1989) at the Technical University of Gdansk. He joined the Department of Electrical Engineering, University of Wyoming, Laramie, in 1989. He is currently with the College of Engineering, University of Idaho, Boise. He was with the Nishizawa Laboratory, Tohoku University, Japan, during 1968–1970, and he spent one year at the Semiconductor Research Institute, Sendai, Japan, as a JSPS Fellow during 1975–1976. He was a Visiting Scholar at Auburn University, Auburn, AL during 1981–1982 and 1995–1996, and a Visiting Professor at the University of Arizona, Tucson, during 1982–1984. He is the author of four textbooks and more than 200 refereed publications. He is also the holder of 27 patents. His main areas of interest are digital hardware, electronics, CAD development, VLSI, network programming, and neuro-fuzzy systems.

Dr. Wilamowski is the Treasurer of the IEEE Industrial Electronics Society and Vice President of the IEEE Neural Networks Council. He is an Associate Editor of the IEEE TRANSACTIONS ON NEURAL NETWORKS, IEEE TRANSACTIONS ON EDUCATION, IEEE TRANSACTIONS ON INDUSTRIAL ELECTRONICS, and *IEEE Industrial Electronics Newsletter*.

Okyay Kaynak (M'80–SM'90) received the B.Sc. (first class honors) and Ph.D. degrees in electronic and electrical engineering from the University of Birmingham, Birmingham, U.K., in 1969 and 1972, respectively.

After spending seven years in industry, in January 1979, he joined the Department of Electrical and Electronic Engineering, Bogazici University, Istanbul, Turkey, where he is presently a Full Professor. He served as the Chairman of the Computer Engineering Department for three years and as the Director of the Biomedical Engineering Institute for one year, Currently, he is the Chairman of the Department of Electrical and Electronic Engineering, the holder of the UNESCO Chair on Mechatronics, and the Director of the Mechatronics Research and Application Center. He has held long-term Visiting Professor/Scholar positions at various institutions in Japan, Germany, the U.S., and Singapore. His current research interests are in the field of intelligent control and mechatronics. He has authored two books and edited two. He has also authored or coauthored more than 100 papers which have appeared in various journals and conference proceedings.

Dr. Kaynak is currently the Vice President of the IEEE Industrial Electronics Society and an Associate Editor of the IEEE TRANSACTIONS ON INDUSTRIAL ELECTRONICS.